2015

Defect-Related Luminescence in Undoped GaN Grown by HVPE

Michael A. Reshchikov
Virginia Commonwealth University, mreshchi@vcu.edu

A Usikov
Nitride Crystals, Inc.

H Helava
Nitride Crystals, Inc.

Yu. Makarov
Nitride Crystals, Inc.

Defect-related Luminescence in Undoped GaN Grown by HVPE

M. A. RESHCHIKOV,[1,4] A. USIKOV,[2,3] H. HELAVA,[2] and YU. MAKAROV[2]

[1] Department of Physics, Virginia Commonwealth University, Richmond, VA 23284, USA.
[2] Nitride Crystals, Inc. 181E Industry Ct., Ste. B, Deer Park, NY 11729, USA.
[3] Saint-Petersburg National Research University of Information Technologies, Mechanics and Optics, 49 Kronverkskiy Ave., 197101 Saint Petersburg, Russia.
[4] email: mreshchi@vcu.edu

ABSTRACT

Hydride vapor phase epitaxy (HVPE) is used for the growth of low-defect GaN. We have grown undoped films on sapphire and investigated them using steady-state and time-resolved photoluminescence (PL). One of the dominant PL bands in high-quality GaN grown by HVPE is the green luminescence (GL) band with a maximum at 2.4 eV. This PL band can be easily recognized in time-resolved PL measurements due to its exponential decay even at low temperatures (< 50 K), with a characteristic lifetime of 1-2 μs. As the temperature increases from 70 to 280 K, the PL lifetime for the GL band increases by an order of magnitude. This unusual phenomenon can be explained in assumption that the electron-capture coefficient for the GL-related defect decreases with temperature as $T^{-2.6}$.

Key words: GaN, HVPE, photoluminescence, defects

INTRODUCTION

GaN is currently used in many light-emitting devices. Another emerging application for this semiconductor material is in high-power electronics, because GaN is expected to have very high breakdown voltage [1-4]. Hydride vapor phase epitaxy (HVPE) allows fast growth of thick templates with a very low density of structural defects. However, relatively high concentrations of uncontrolled point defects are currently the main obstacle impending the use of GaN in high-power devices. In spite of many years of research, most of the defects in undoped GaN remain unidentified. The identification of point defects is also necessary for the development of first-principles calculation methods. Photoluminescence (PL) is a powerful tool for the investigation of point defects, which is especially useful in wide-bandgap semiconductors such as GaN.

The most common defect-related PL band in high-purity GaN templates is the green luminescence (GL) band with a maximum at about 2.4 eV at low temperatures [5-9]. The GL band is also strong in bulk GaN grown from solution [10,11]. In different undoped GaN layers grown by HVPE, other defect-related PL bands include the red luminescence (RL) band with a maximum at 1.8 eV [9,13-15], the yellow luminescence (YL) band at 2.2 eV [5,8,9,14], the blue luminescence (BL) band at 2.9 eV [14,16], and the ultraviolet luminescence (UVL) band with the main peak at 3.26 eV [5,13,16,17]. The latter should not be confused with PL bands related to structural defects such as stacking faults [18-20], which can be observed in the same spectral region but have different shape, position, and the strength of electron-phonon coupling [5]. In this work, we analyze PL from point defects in undoped, high-quality GaN layers grown by HVPE on sapphire substrates. Particular attention is given to the GL band since it demonstrates unusual properties.

EXPERIMENTAL DETAILS

Undoped 10-30 μm-thick GaN films were grown by HVPE on c-plane 2-inch sapphire substrates. The growth was performed at atmospheric pressure in argon ambient. Ammonia and hydrogen chloride (HCl) were used as precursors. For GaN growth, HCl was passed over the Ga source producing gallium chlorides in the vapor phase of the source zone. The chlorides were transferred by argon gas to the growth zone. The reaction between the ammonia and the gallium chlorides in the growth zone produced the GaN layer on the substrate. The growth rate was controlled by the HCl gas flow rate through the metallic sources. The quartz reactor design allowed growth of multilayer structures either by varying the precursor gas flows or by transferring the substrate between a growth zone and a dwell zone kept at the same temperature. The growth was performed at temperatures of 850-1000 ^{o}C which are somewhat lower than in a typical HVPE process (1020 – 1040 ^{o}C). The growth was initiated at low growth rate and then continued with an increased growth rate of about 0.2–1 μm/min. The room-temperature concentration of free electrons in these samples is between 2×10^{16} and 4×10^{17} cm^{-3}, as was determined from analysis of the temperature-dependent Hall-effect measurements.

Steady-state and time-resolved PL was excited with He-Cd and N lasers, respectively. Calibrated neutral-density filters were used to attenuate the excitation power density (P_{exc}) over the range 10^{-3} - 0.3 W/cm^2. Other details can be found in Ref. [21].

RESULTS

Typical PL spectra at low excitation intensity are shown in Fig. 1. At 18 K, the exciton emission includes a strong donor-bound exciton line at 3.476 eV with a full width at half maximum (FWHM) of 3.5 meV and a free exciton line at 3.482 eV. A blue shift by about 5 meV

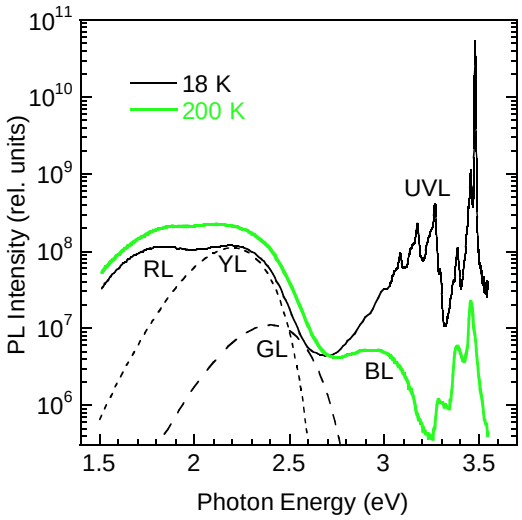

Fig. 1. Steady-state PL spectra at 18 and 200 K and P_{exc} = 10^{-3} W/cm^2 for sample 1007. The PL intensity is divided by the excitation intensity. Dashed lines indicate contributions of the YL and GL bands to the spectrum at 18 K calculated using Eq. (1) with the following fitting parameters: S_e = 7.4, E_0 = 2.64 eV, $\hbar\omega_{\max} = 2.2$ eV, $\hbar\Omega_e = 52$ meV for the YL band and S_e = 8.5, E_0 = 2.9 eV, $\hbar\omega_{\max} = 2.4$ eV, $\hbar\Omega_e = 41$ meV for the GL band.

is caused by strain in GaN grown on sapphire substrate. Five defect-related PL bands could be resolved by changing the temperature or excitation intensity: the UVL band with the strongest peak at 3.265 eV followed by a few LO phonon replicas, the Zn-related BL band with a maximum at 2.9 eV, the GL band with a maximum at 2.4 eV, the YL band with a maximum at 2.2 eV, and the RL band with a maximum at 1.8 eV. The Zn-related BL band can be observed in the steady-state PL spectrum only at temperatures between 150 and 200 K (Fig. 1), when the UVL band is quenched, while the quenching of the BL band does not start [5]. The source of Zn in HVPE-grown GaN could be Ga metal contamination and/or the "memory effect" when Zn-doping was used in an HVPE reactor.

The YL and GL bands in HVPE-grown GaN were studied in detail in Ref. [22]. The changes in shape, position and intensity were insignificant for these PL bands as the temperature increased from 18 to 100 K. The shapes of the YL and GL bands were simulated with the following expression [23]:

$$I^{PL}(\hbar\omega) \propto \exp\left[-2S_e\left(\sqrt{\frac{E_0 + 0.5\hbar\Omega_e - \hbar\omega}{E_0 + 0.5\hbar\Omega_e - \hbar\omega_{\max}}} - 1\right)^2\right], \quad (1)$$

where S_e and $\hbar\Omega_e$ are the Huang-Rhys factor and the dominant phonon energy for the excited state, $\hbar\omega$ and $\hbar\omega_{\max}$ are the photon energy and the energy of the PL band maximum, and E_0 is the zero-phonon line (ZPL) energy. The parameters used in the fit are given in the caption to Fig. 1. The parameter $\hbar\Omega_e$ was determined from the temperature dependence of the PL band FWHM [5]. Other parameters were chosen to fit the shapes of the YL and GL bands in PL spectra from samples where these PL bands were dominant and had small overlap with other PL bands. The contribution of the GL band to the PL spectrum at 18 K is almost negligible at low excitation intensity (Fig. 1). However, due to a superlinear increase of this band intensity with the excitation intensity, its contribution to the spectrum at P_{exc} = 0.3 W/cm^2 becomes significant (Fig. 2).

In time-resolved PL measurements, the GL band was clearly observed at time delays from 10^{-7} to 10^{-6} s after the laser pulse (Fig. 3). For longer time delays, the YL band with a maximum at 2.2 eV or the RL band with a maximum at 1.8 eV became the dominant PL bands due to their long lifetime (milliseconds). Figure 4(a) shows the decay of the GL intensity (at 2.4 eV) after a laser pulse at selected temperatures. The dependences can be fit with the following expression

$$I^{PL}(t) = I^{PL}(0)\exp\left(-t/\tau\right), \quad (2)$$

where τ is the PL lifetime. The deviation of the experimental dependences from the pure exponential dependences [shown with lines in Fig. 4(a)] can be explained by appearance of the YL band at longer time delays, see Fig. 3. As the temperature increases from 100 to 260 K, the PL lifetime of the GL band increases from 4 to 54 μs, and the peak intensity (at t = 0) decreases by the same factor. Figure 4(b) shows the product of the PL intensity and elapsed time plotted as

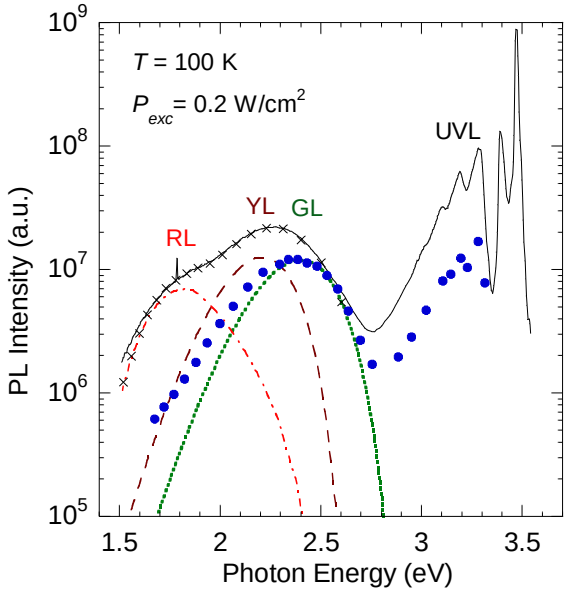

Fig. 2. Steady-state PL spectrum at 100 K and P_{exc} = 0.2 W/cm^2 for sample 1007. The PL intensity is divided by the excitation intensity. The dashed and dotted lines indicate contributions of the RL, YL, and GL bands to the spectrum. The shapes of the YL and GL bands are simulated using Eq. (1) with the parameters given in the caption to Fig. 1. The shape of the RL band is reproduced from a typical RL band spectrum at 100 K in GaN samples where the RL band was the dominant defect-related band [13]. Superposition of the simulated spectra of the RL, YL, and GL bands is shown with ×'s. Closed circles show the PL spectrum measured in time-resolved PL measurements (at time delay of 3×10^{-7} s after the laser pulse) and shifted arbitrarily in the vertical direction to demonstrate an agreement between the simulated GL band and the GL band observed in time-resolved PL measurements.

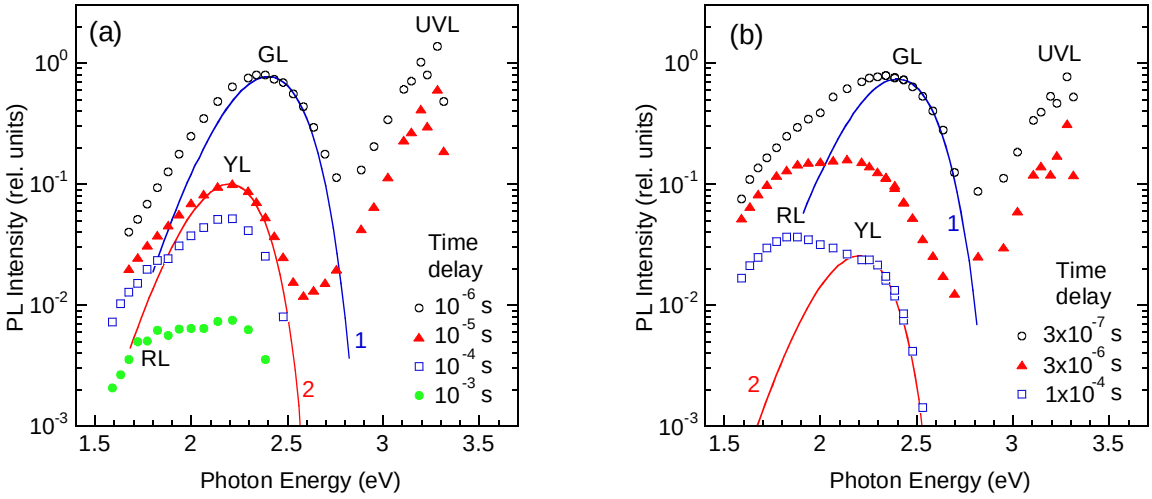

Fig. 3. Time-resolved PL spectra at 100 K. (a) Sample 1007. (b) Sample H201. The symbols show the PL intensity at indicated time delays after a laser pulse. The spectra are normalized so that the peak intensity of the GL band is equal to one at t = 0.The solid lines are calculated shapes for the GL band (1) and the YL band (2) using Eq. (1) with the parameters given in the caption to Fig. 1.

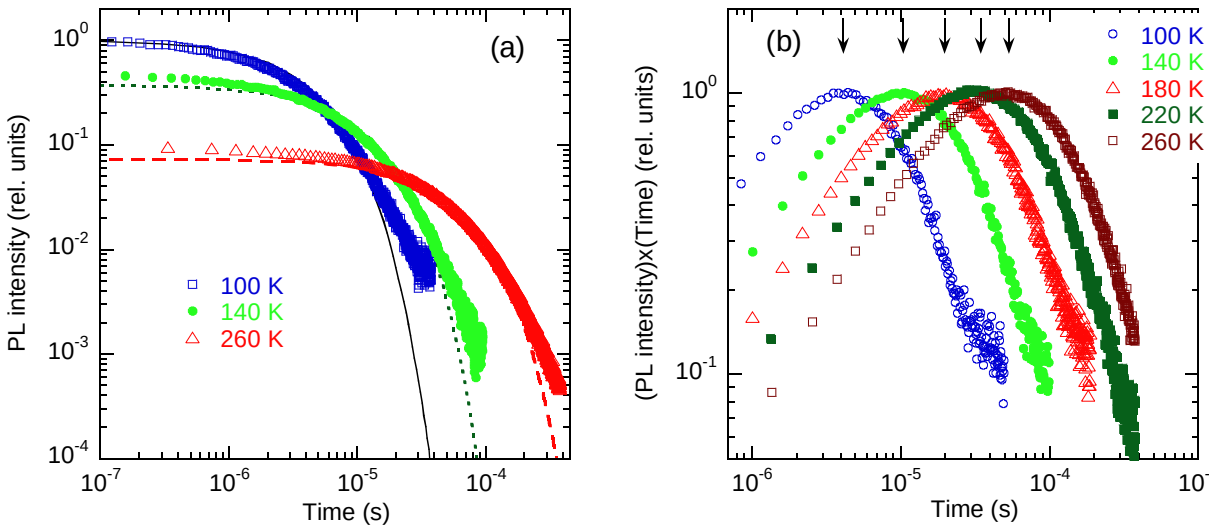

Fig. 4. (a) Decay of the GL band intensity (at photon energy of 2.4 eV) after a pulse excitation at selected temperatures for sample RS280. The dependences are normalized so that the intensity of the GL band at 100 K is equal to one at $t = 0$. Every 10^{th} point is shown. The lines are the fits using Eq. (2) with the following parameter τ : 4 μs (100 K), 10.5 μs (140 K), 54 μs (260 K). (b) Normalized product of the PL intensity and time after a laser pulse. Every 30^{th} point is shown. Arrows indicate the effective lifetimes found as the maxima of these dependences.

a function of time delay. Following an approach suggested in Ref. [24], the effective lifetime of PL, τ, is defined as the position of the maximum in this dependence [shown with arrows in Fig. 4(b)].

The temperature dependences of τ for the UVL and GL bands are shown in Fig. 5(a). The PL lifetime for the UVL band decreases from 100 to 20 μs as the temperature increases from 50 to 100 K. At higher temperatures, the PL lifetime of the UVL band decreases exponentially due to the quenching of the UVL band (not shown) [25]. After a laser pulse, the PL is expected to decay exponentially in the case of transitions of electrons from the conduction band to a defect level, with a characteristic lifetime given by the expression [5,25]

$$\tau = \frac{1}{nC_{nA}}, \qquad (3)$$

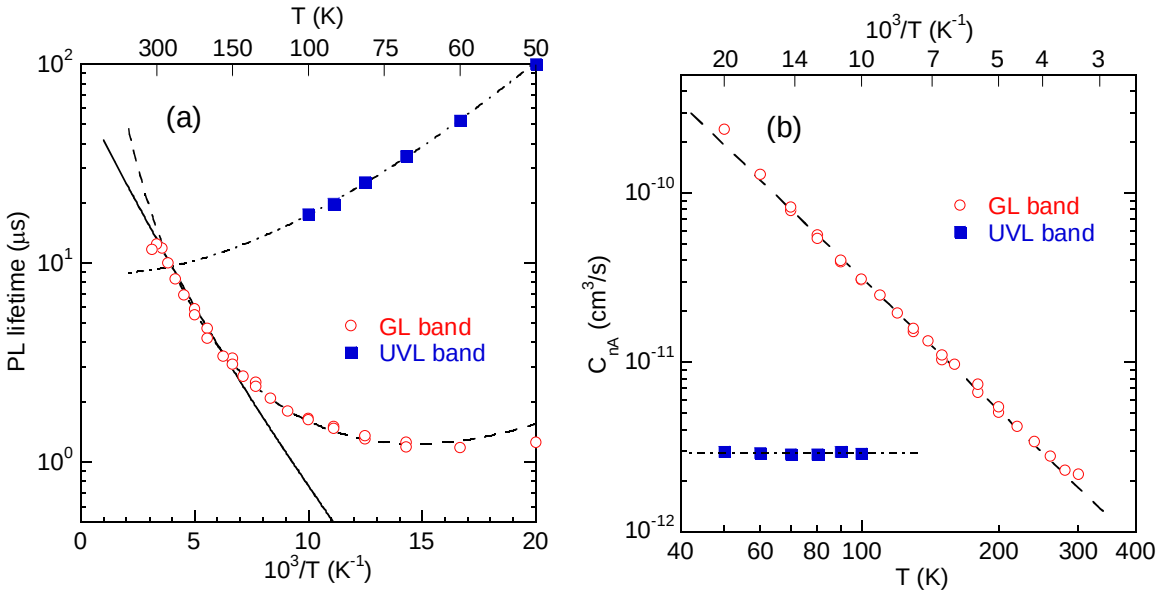

Fig. 5. Temperature dependences of PL lifetime and the electron-capture coefficient for the UVL and GL bands in sample 1007. (a) PL lifetime as a function of inverse temperature (logarithmic scale). (b) Electron capture coefficient (log-log scale). The symbols are experimental data from time-resolved PL measurements. The lines indicate fits using Eq. (3) in which the temperature dependence of n is simulated using Eq. (4) with $N_D = 6\times10^{16}$ cm^{-3}, $N_A = 2\times10^{16}$ cm^{-3}, $E_D = 16$ meV, and $g = 2$. The dash-dotted line for the UVL band is calculated using Eq. (3) with $C_{nA} = 2.9\times10^{-12}$ cm^3/s [both in (a) and (b)]. The dashed line for the GL band is calculated using Eq. (3) with $C_{nA} = 5\times10^{-6}T^{-2.6}$ cm^3/s [both in (a) and (b)]. The solid line for the GL band is calculated using Eq. (3) with $C_{nA} = 3.6\times10^{-13}\exp(E/kT)$ cm^3/s and $E = 45$ meV.

where n is the concentration of free electrons and C_{nA} is the electron-capture coefficient. The temperature dependence of n was simulated with the following expression [26]:

$$n = \sqrt{(n_1 + N_A)^2 / 4 + n_1(N_D - N_A)} - (n_1 + N_A)/2, \tag{4}$$

with

$$n_1 = N_c g^{-1} \exp(-E_D / kT). \tag{5}$$

Here, N_D and N_A are the concentrations of the shallow donors and all acceptors, respectively, N_c is the effective density of states in the conduction band, g is degeneracy of the shallow donor level, E_D is the ionization energy of the shallow donor, and k is Boltzmann's constant.

The temperature dependence of the PL lifetime for the UVL band is fit in Fig. 5(a) using Eq. (3) with a constant coefficient C_{nA} (2.9×10^{-12} cm^3/s). The PL lifetimes for the BL and YL bands also decreased as the temperature increased, similar to the behavior of the UVL band. The agreement of the experimental dependences with the theoretical dependences calculated using Eq. (3), in which the coefficient C_{nA} is a constant, indicates that transitions of electrons from the conduction band to the defect levels are responsible for these PL bands.

In contrast to the above behavior, the PL lifetime of the GL band has a weak temperature dependence between 50 and 100 K and *increases* by about an order of magnitude as the temperature increases from 100 to 300 K [Fig. 5(a)]. The largest slope of this increase (at 150 K < T < 280 K) corresponds to the activation energy, E, of about 50 meV. The analysis of time-resolved PL for several GaN samples having different concentrations of free electrons indicates that the PL lifetime for the GL band in this temperature range is inversely proportional to the concentration of free electrons, while the PL lifetime at T < 100 K is about the same for all the samples. Such behavior was explained assuming that at T < 100 K the GL band is caused by transitions of electrons from an excited state located near the conduction band minimum to the ground state located at about 0.5-0.6 eV above the valence band maximum [5]. At T > 100 K, transitions of electrons from the conduction band to the same defect level become dominant, because the thermal emission of electrons from the excited state to the conduction band becomes significant. By using Eq. (3) and the temperature dependence of the concentration of free electrons, the temperature dependence of the coefficient C_{nA} is found [Fig. 5(b)]. As can be seen from this figure, the temperature dependence of C_{nA} for the GL band can be well fit with a power law of the form $C_{nA} \propto T^{-n}$ with n = 2.6.

At T > 280 K, the lifetime of the GL band decreases very similar to the temperature dependence of the PL intensity, I^{PL}. Figure 6 shows the $\tau(T)$ and $I^{PL}(T)$ dependences for a sample with the strongest GL band. The GL intensity is quenched in agreement with the prediction of the phenomenological model [27],

$$I^{PL}(T) = \frac{I^{PL}(0)}{1+(1-\eta_0)\tau_0 C_{pA} N_v g^{-1} \exp\left(-E_A / kT\right)}, \quad (6)$$

where N_v is the effective density of states in the valence band, C_{pA} is the hole-capture coefficient for the defect level responsible for the GL band, g is the degeneracy of this level (assumed to be equal to 2), and E_A is the distance between this level and the top of the valence band. In this equation, τ_0 is the PL lifetime not accounting for the PL quenching effect (usually the value just before quenching) [27]. The temperature dependence of the PL lifetime is described with the same equation, in which $I^{PL}(T)$ and $I^{PL}(0)$ are replaced with $\tau(T)$ and τ_0, respectively [25]. In Ref. [22] we assumed that τ_0 is a constant (40 μs for this sample), and from the fit of the

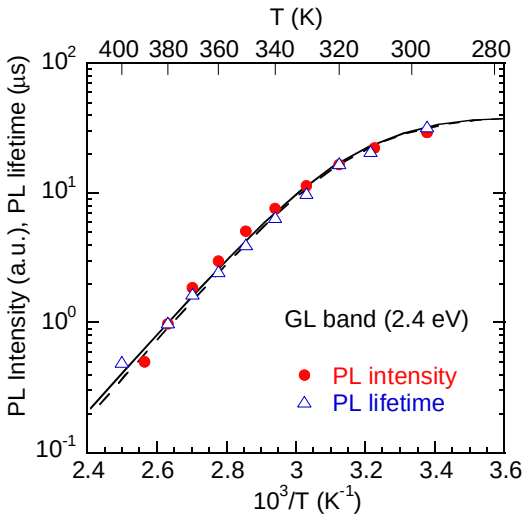

Fig. 6. Temperature dependence of the GL band intensity and the GL lifetime for GaN sample B73. The symbols are the experimental data from Ref. [22]. The solid line is calculated using Eq. (6) with the following parameters: η_0 = 0.1, C_{pA} = 10^{-6} cm^3/s, E_A = 505 meV, N_v = $3.2\times10^{15}T^{3/2}$ cm^{-3}, g = 2, τ_0 = $(C_{nA}\, n)^{-1}$ with C_{nA} = $3.6\times10^{-13}\exp(-E/kT)$ cm^3/s and E = 45 meV. The dashed line is calculated using Eq. (6) with the same parameters except for the following: C_{pA} = 3×10^{-7} cm^3/s, E_A = 475 meV, and C_{nA} = $5\times10^{-6}T^{-2.6}$ cm^3/s.

experimental data with Eq. (6) obtained C_{pA} = 10^{-6} cm^3/s and E_A = 535 meV. However, the temperature dependence of τ_0 between 280 and 400 K due to the temperature-dependent electron-capture coefficient will affect the parameters C_{pA} and E_A, because the PL intensity (and PL lifetime τ) is proportional to $\left[\tau_0 C_{pA} \exp\left(-E_A / kT\right)\right]^{-1}$ in the region of PL quenching. The extrapolation of the exponential dependence of τ_0 (with E = 45 meV) to temperatures higher than 280 K [the solid line in Fig. 5(a)] results in the decrease of E_A from 535 to 505 meV for the best fit, with C_{pA} = 10^{-6} cm^3/s (the solid line in Fig. 6). When the temperature dependence of τ_0 is extrapolated assuming that $C_{nA}(T) \propto T^{-2.6}$ at T > 280 K [the dashed line in Fig. 5(a)], the best fit gives E_A = 475 meV and C_{pA} = 3×10^{-7} cm^3/s (the dashed line in Fig. 6, which is almost indistinguishable from the solid curve).

DISCUSSION

Five defect-related PL bands can be resolved by changing temperature or excitation intensity and using time-resolved or steady-state PL (Figs. 1-3). As for the defects responsible for these PL bands, only the BL band with a maximum at 2.9 eV is unambiguously identified as arising from transitions via the Zn_{Ga} acceptor [5]. We focus on the GL band because it is the dominant PL band in high-quality GaN grown by HVPE and because it demonstrates unusual behavior. Namely, the effective lifetime of this PL band increases as the temperature increases from 100 to 280 K, while it is expected to decrease for PL bands related to transitions of electrons from the conduction band to a defect level [Fig. (5(a)]. This increase can be attributed to the decrease of the electron-capture coefficient. Then, $C_{nA} \propto T^{-2.6}$ for the GL band [Fig. 5(b)]. Interestingly, a similar dependence, $C_{nA} \propto T^{-3}$, is expected for the capture of electrons by positively charged donors in Ge and Si [28]. However, this is only the case for nonradiative transitions, and for

radiative transitions no temperature dependence of the capture coefficients is expected [29]. Experimentally, we observe temperature-independent C_{nA} for the RL, YL, BL, and UVL bands in GaN. The latter is shown in Fig. 5(b).

Currently, we are unable to construct a comprehensive model which would explain consistently all the existing experimental data for the GL band in GaN. In Ref. [22], we assigned the GL band to the 0/+ charge state of the isolated C_N defect. Further theoretical research is needed to confirm or disprove the assignment and explain the experimental results presented in this work.

CONCLUSIONS

We have observed five defect-related PL bands in undoped GaN grown by HVPE on sapphire substrates. The PL bands can be resolved in the steady-state or time-resolved PL spectra by changing temperature or excitation intensity, as well as by recording PL spectra at different time delays after a laser pulse. The PL lifetime of the RL, YL, BL, and UVL bands decreases with increasing temperature due to the increase of the concentration of free electrons. The electron-capture coefficient for these transitions is temperature-independent. In sharp contrast, the effective lifetime of the GL band increases by an order of magnitude as the temperature increases from 100 to 280 K. This unusual behavior can be explained by a power dependence of the corresponding electron-capture coefficient of the form $C_{nA} \propto T^{-2.6}$.

ACKNOWLEDGEMENT

M.R. acknowledges support from the National Science Foundation (DMR-1410125).

REFERENCES

1. Y. Saitoh, K. Sumiyoshi, M. Okada, T. Horii, T. Miyazaki, H. Shiomi, M. Ueno, K. Katayama, M. Kiyama, and T. Nakamura, Appl. Phys. Express **3**, 081001 (2010).

2. Y. Wang, H. Xu, S. Alur, Y. Sharma, F. Tong, P. Gartland, T. Issacs-Smith, C. Ahyi, J. Williams, M. Park, G. Wheeler, M. Johnson, A. A. Allerman, A. Hanser, T. Paskova, E. A. Preble, and K. R. Evans, Phys. Stat. Sol. (c) **8**, 2430 (2011).

3. J. Everts, J. van den Keybus, M. Van Hove, D. Visalli, P. Srivastava, D. Marcon, Kai Cheng, M. Leys, S. Decoutere, J. Driesen, and G. Borghs, Electron Device Letters, IEEE **32**, 1370 (2011).

4. M.-W. Ha, C. H. Roh, D. W. Hwang, H. G. Choi, H. J. Song, J. H. Lee, J. H. Park, O. Seok, J. Lim, M.-K. Han, and C.-K. Hahn, Jap. J. Appl. Phys. **50**, 06GF17 (2011).

5. M. A. Reshchikov and H. Morkoç, J. Appl. Phys. **97**, 061301 (2005).

6. E. R. Glaser, J. A. Freitas, Jr., G. C. Braga, W. E. Carlos, M. E. Twigg, A. E. Wickenden, D. D. Koleske, R. L. Henry, M. Leszczynski, I. Grzegory, T. Suski, S. Porowski, S. S. Park, K. Y. Lee, and R. J. Molnar, Physica B **308-310**, 51 (2001).

7. A. Y. Polyakov, I.-H. Lee, N. B. Smirnov, A. V. Govorkov, E. A. Kozhukhova, and S. J. Pearton, J. Appl. Phys. **109**, 123701 (2011).

8. J. A. Freitas, Jr., M. A. Mastro, E. R. Glaser, N. Y. Garces, S. K. Lee, J. H. Chung, D. K. Oh, and K. B. Shim, J. Crystal Growth **350**, 27 (2012).

9. P. P. Paskov, B. Monemar, T. Paskova, E. A. Preble, A. D. Hanser, and K. R. Evans, Phys. Stat. Sol. (c) **6**, S763 (2009).

10. N. Y. Garces, B. N. Feigelson, J. A. Freitas, Jr., J. Kim, R. Myers-Ward, and E. R. Glaser, J. Crystal Growth **312**, 2558 (2010).

11. J. A. Freitas, Jr., J. G. Tischer, N. Y. Garces, and B. N. Feigelson, J. Crystal Growth **281**, 168 (2005).

12. F. Tuomisto, K. Saarinen, B. Lucznik, I. Grzegory, H. Teisseyre, T. Suski, S. Porowski, P. R. Hageman, and J. Likonen, Appl. Phys. Lett. **86**, 031915 (2005).

13. M. A. Reshchikov, A. Usikov, H. Helava, and Yu. Makarov, Appl. Phys. Lett. **104**, 032103 (2014).

14. A. Castaldini, A. Cavallini, L. Polenta, C. Diaz-Guerra, and J. Piqueras, J. Phys.: Condens. Matter **14**, 13095 (2002).

15. W. Götz, L. T. Romano, B. S. Krusor, and N. M. Johnson, Appl. Phys. Lett. **69**, 242 (1996).

16. J. A. Freitas, Jr., J. Crystal Growth **281**, 168 (2005).

17. B. Monemar, P. P. Paskov, F. Tuomisto, K. Saarinen, M. Iwaya, S. Kamiyama, H. Amano, I. Akasaki, and S. Kimura, Physica B **376-377**, 440 (2006).

18. R. Liu, A. Bell, F. A. Ponce, C. Q. Chen, J. W. Yang, and M. A. Khan, Appl. Phys. Lett. **86**, 021908 (2005).

19. I. Tischer, M. Feneberg, M. Schirra, H. Yacoub, R. Sauer, K. Thonke, T. Wunderer, F. Scholz, L. Dieterle, E. Müller, and D. Gerthsen, Phys. Stat. Sol. B **248**, 611 (2011).

20. P. P. Paskov, R. Schifano, T. Malinauskas, T. Paskova, J. P. Bergman, B. Monemar, S. Figge, D. Hommel, B. A. Haskell, P. T. Fini, J. S. Speck, and S. Nakamura, Phys. Stat. Sol. (c) **3**, 1499 (2006).

21. M. A. Reshchikov, A. Kvasov, T. McMullen, M. F. Bishop, A. Usikov, V. Soukhoveev, and V. A. Dmitriev, Phys. Rev. B **84**, 075212 (2011).

22. M. A. Reshchikov, D. O. Demchenko, A. Usikov, H. Helava, and Yu. Makarov, Phys. Rev. B (paper BT12815, accepted on 11/05/2014).

23. M. A. Reshchikov, D. O. Demchenko, J. D. McNamara, S. Fernández-Garrido, and R. Calarco, Phys. Rev. B **90**, 035207 (2014).

24. R. Y. Korotkov, M. A. Reshchikov, and B. W. Wessels, Physica B **325**, 1 (2003).

25. M. A. Reshchikov, J. Appl. Phys. **115**, 103503 (2014).

26. D. K. Schroder, *Semiconductor Material and Device Characterization*, 3rd Edition, John Wiley and Sons, Hoboken, NJ, 2006.

27. M. A. Reshchikov and R. Y. Korotkov, Phys. Rev. B **64**, 115205 (2001).

28. V. N. Abakumov, V. I. Perel, and I. N. Yassievich, *Nonradiative Recombination in Semiconductors*, Elsevier, Amsterdam, 1991; V. N. Abakumov, V. I. Perel, and I. N. Yassievich, Sov. Phys. Semicond. **12**, 1 (1978).

29. J. I. Pankove, *Optical Processes in Semiconductors*, Dover Publ., Inc., New York, 1971.